

TRANSPARENT ZnO-BASED OHMIC CONTACT TO p-GaN

E. Kaminska¹, A. Piotrowska¹, K. Golaszewska¹, M. Guzewicz¹, R. Kruszka¹, A. Kudla¹, T. Ochalski¹, A. Barcz^{1,2}, T. Dietl², F. Matsukura^{2,3}, M. Sawicki², A. Wawro², M. Zielinski², J. Jasinski⁴, Z. Liliental-Weber⁴

¹Institute of Electron Technology, Al. Lotnikow 46, 02-668 Warsaw, Poland

²Institute of Physics, PAS, Al. Lotnikow 46, 02-668 Warsaw, Poland

³Research Institute of Electrical Communication, Tohoku University, Sendai 980-8577, Japan

⁴Lawrence Berkeley National Laboratory, Berkeley, CA 94720, U.S.A.

ABSTRACT

Highly conductive ZnO films were fabricated on p-GaN in a two-step process. First, zinc was thermally evaporated on p-GaN. Next, zinc film was oxidized in oxygen flow. To increase the conductivity of ZnO, nitrogen was introduced into zinc during its deposition. The above procedure proved successful in fabricating ZnO of the resistivity of $\sim 1 \times 10^{-3} \Omega \text{cm}$ and resulted in ohmic contacts of resistivity $\sim 1 \times 10^{-2} \Omega \text{cm}^2$ to low-doped p-GaN, and light transmittance of $\sim 75\%$ in the wavelength range of 400-700 nm.

INTRODUCTION

In a variety of optoelectronic applications, such as light-emitting, -detecting and -triggered semiconductor devices the top electrode serves as both ohmic contact and optical window. For GaN-based photonic devices, where the major losses of performance are due to poor conductivity of p-type subcontact region, causing the so-called “current crowding” problem, a highly conductive and transparent p-type electrode is a prerequisite. Among the investigated metallizations that would allow low-resistivity contact to p-GaN, oxidized Ni/Au bilayer was reported to give the lowest operating voltages [1-3]. For the transparent p-type electrode, optimization of Ni/Au metallization via reducing its thickness [4,5] has been achieved, however, at the cost of increase of the specific contact resistance. Another approach for obtaining effective current-spreading layer, providing low-resistivity contact to p-type GaN in conjunction with efficient and uniform light emission, would be to make the p-type contact/window layer from a transparent conducting oxide (TCO). Following this approach, indium tin oxide (ITO) films have been recently tested as electrical contacts to p-side of GaN-based light emitting diode (LED), vertical cavity laser (VCSEL) and resonant cavity LED, allowing satisfactory lateral current spreading and required transparency [6,7]. Below, we report on the use of ZnO as an ohmic contact to p-GaN. This material is an excellent candidate for a thermally stable heterojunction contact to p-GaN. Both materials possess the same wurtzite structure with small lattice mismatch. As compared to ITO, ZnO offers higher chemical stability at higher temperatures [8, 9]. The transport properties of ZnO depend strongly upon the stoichiometry and on the nature and concentration of impurities and dopants introduced into the film [9]. Usually, ZnO films are fabricated by sputtering [10] or pulsed laser-deposition [8, 9]. New idea of this work is to form highly conductive ZnO films in a two-step process: first, thin film of elemental Zn is deposited on p-GaN substrate by thermal evaporation in high vacuum. Next, Zn film is oxidized in an oxygen flow. To increase the doping level, a controlled amount of dopant was introduced into Zn during its deposition.

EXPERIMENTAL DETAILS

The substrate materials for this study were 2 μm thick either Mg doped p-GaN ($p = 1 \times 10^{17} \text{cm}^{-3}$) or undoped GaN epilayers, grown by MOCVD on sapphire. For optical measurements double-side polished sapphire substrates were employed.

During the deposition of Zn, nitrogen as a dopant species was bled into vacuum chamber by means of a regulated valve, at a partial pressure from the range 1×10^{-4} - 4×10^{-6} Torr. To promote uniform condensation of Zn on non-metallic substrates, an Au nucleation film was predeposited. Zn films of a thickness 50-100 nm were used in our experiments. The oxidation of Zn was carried out by furnace annealing in O_2 flow, at 300-320 $^\circ\text{C}$, i.e. 20-40 $^\circ\text{C}$ below the sublimation temperature of Zn [11]. Finally, 200 nm thick Au or Pt overlayer for contacting purposes was deposited, and samples were patterned for electrical measurements. In order to avoid the incorporation of uncontrolled impurities, only high purity materials (99,999%) were used in fabrication of ZnO films.

The transport properties of thin ZnO films were assessed from measurements of sheet resistance by four-point probe, and using van der Pauw method. Ohmic contacts were characterized by circular transmission line method (CTLM) [12]. The dimensions, in notation [12], were: $r_0=30 \mu\text{m}$, $r_1=54 \mu\text{m}$, $r_1'=85 \mu\text{m}$, $r_2=138 \mu\text{m}$, $r_2'=174 \mu\text{m}$. Measurements were carried out using Keithley 2400 SourceMeter. Optical transmission of the films was measured by means of monochromatically dispersed light of quartz-tungsten-halogen lamp. Intensity of transited light was detected by using Si photodiode biased in reversed polarization. Optical parameters of the ZnO layers were determined with Woollam VASE spectroscopic ellipsometer. Measurements were done at two angles 65 $^\circ$ and 75 $^\circ$. The surface morphology of ZnO films was characterized by atomic force microscopy (AFM). The microstructure of contacts was investigated by cross-sectional transmission electron microscopy (XTEM) and high resolution imaging (HREM) combined with energy dispersive x-ray spectroscopy (EDX). TEM observations were performed using a Topcon 002B microscope operating at 200 keV. EDX studies were done using Philips CM200 microscope. A microprobe size of 1.4 nm was used for EDX analysis. Fast Fourier transform (FFT) of HREM images were used to identify crystalline phases. SIMS profiling was performed with a Cameca 6F instrument with a cesium primary ion beam and detection of CsMi+ secondary cluster ions.

RESULTS AND DISCUSSION

Electrical properties

Resistivity of oxidized zinc films as a function of the partial pressure of N_2 during zinc deposition is plotted in figure 1(a). While the nominally undoped ZnO films were highly resistive, by introducing nitrogen into the deposition chamber it was possible to decrease the resistivity down to $1 \times 10^{-3} \Omega\text{cm}$. Hall effect measurement performed on low-resistivity samples showed that the material is n-type and degenerately doped. The thickness of oxidized zinc films was ~ 1.2 times higher as compared to the as-deposited ones. The typical I-V characteristic of p-GaN/ZnO/Au contact is shown in figure 1(b). As-deposited contacts exhibited linear I-V behavior. The resistivity of contacts formed on low-doped p-type GaN ($p=1 \times 10^{17} \text{cm}^{-3}$) was $1-2 \times 10^{-2} \Omega\text{cm}^2$.

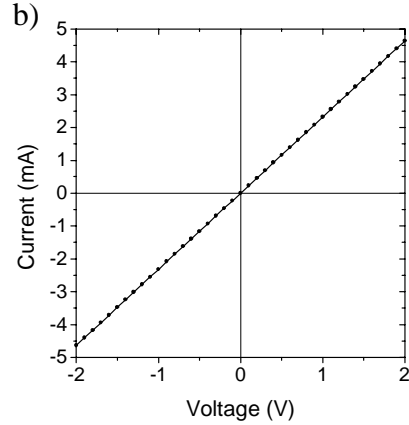
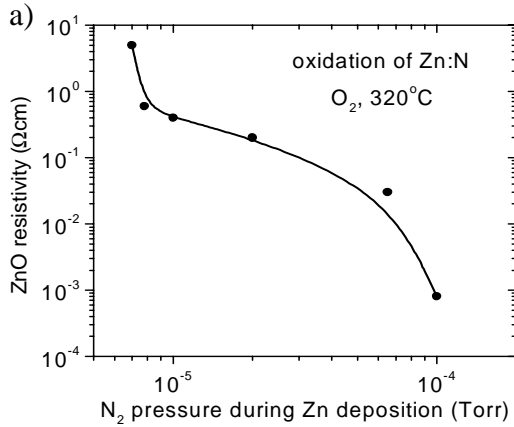


Figure 1. (a) Resistivity of ZnO as a function of N₂ partial pressure during the deposition of Zn and (b) I-V characteristic of the as-deposited p-GaN/ZnO/Au contact.

Optical properties

In figure 2 are presented refraction n and extinction k indices as a function of wavelength in 240-1100 nm spectral range. 120 nm thick ZnO films show an average transmission of about 75% for wavelengths between 400 and 700 nm, as given in figure 3.

Contact microstructure

As analyzed by AFM, nuclei of gold form at the surface of GaN regularly shaped grains, ~5 nm in size. Deposition of zinc resulted in the RMS roughness of 7.35 nm. The size of zinc grains was 40-50 nm. Upon oxidation grains slightly grew, and the surface roughened up to 11.3 nm. The surface morphology of oxidized zinc film on GaN is presented in figure 4.

Figures 5(a) and (b) are SIMS profiles showing the elemental composition of the uniformly oxidized zinc films on GaN and sapphire substrates. Although the presence of nitrogen can be inferred from the step in the profile occurring within the ZnO film deposited on GaN, the signal is partially masked by the N contribution from the semiconductor. Therefore, similar metallization was prepared on a sapphire substrate where the N content is clearly seen.

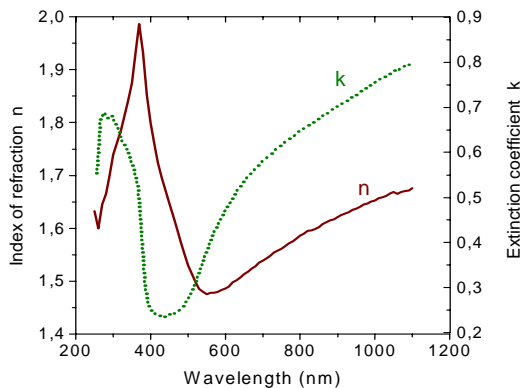


Figure 2. Refraction and extinction indices of ZnO.

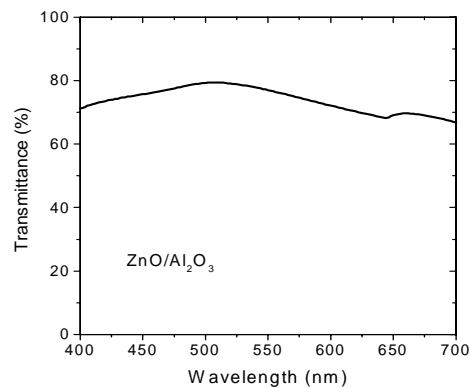


Figure 3. Transmittance of ZnO film as a function of wavelength.

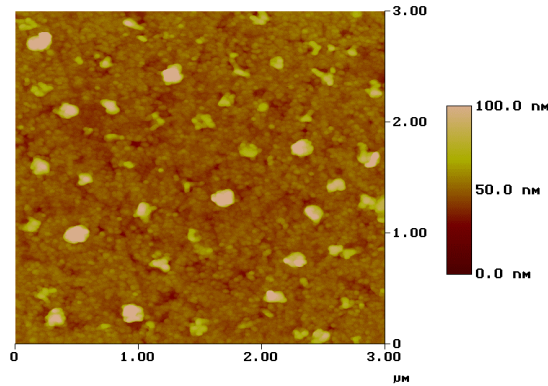


Figure 4. AFM image of the surface of oxidized Zn film.

The microstructure of the as-deposited GaN/Zn contact, shown in figure 6(a), consists of two distinct films. As inferred from EDX analysis, the first, interfacial one, is composed of Au and Zn, the second being Zn. TEM analysis of the GaN/oxidized zinc interface, given in figure 6(b), shows an intact initial surface of GaN, adjacent to which elongated (20-40 nm) grains are visible. These are embedded in a continuous overlayer. High resolution analysis assisted by fast Fourier transform procedure (FFT), performed on the above described distinct areas, made it possible to identify the islands as gold, and the main layer as crystalline zinc oxide. HREM images and corresponding FFTs are presented in figure 6(c).

CONCLUSIONS

We have successfully developed a fabrication method of high conductivity, transparent zinc oxide and have applied it to manufacturing of a transparent ohmic contact to p-type GaN. It was found that electrical properties ZnO thin films, formed by thermal evaporation of zinc and consecutive zinc oxidation, could be precisely controlled by varying the partial pressure of nitrogen, introduced into the zinc deposition chamber.

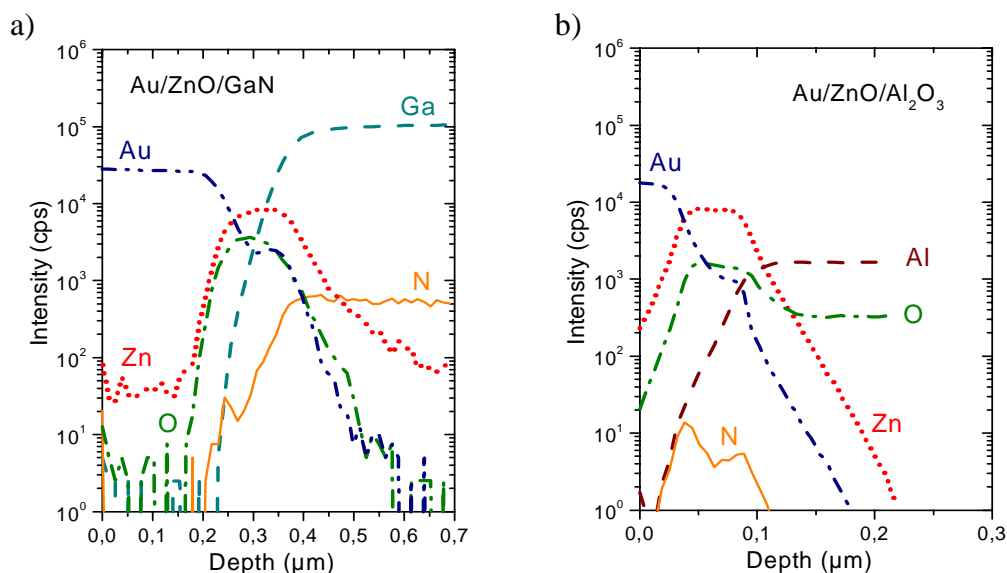


Figure 5. SIMS profiles of ZnO/Au contacts manufactured on (a) GaN or (b) sapphire substrates.

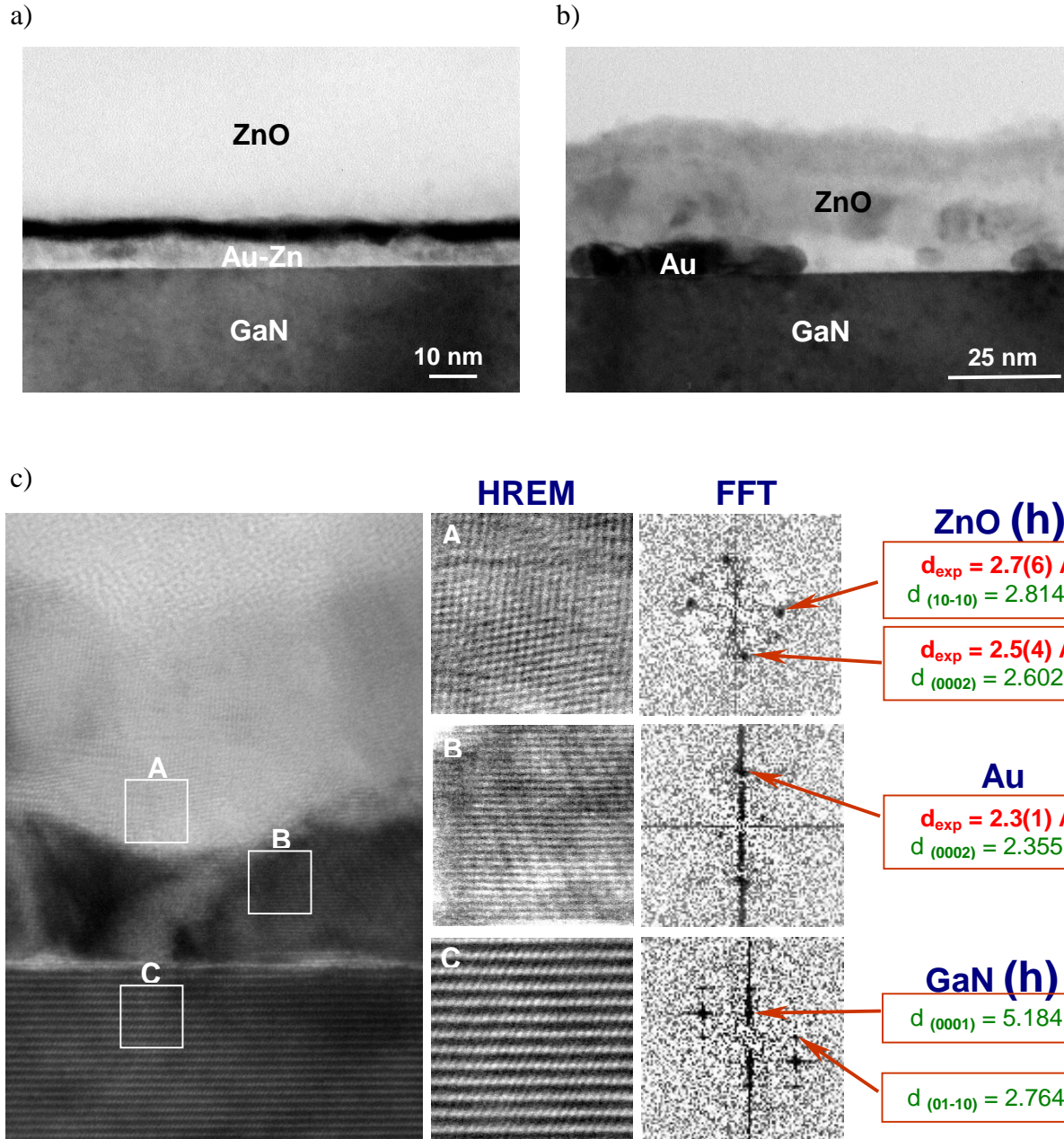


Figure 6. TEM micrographs of GaN/Zn interface: (a) as-deposited, (b) after oxidation, (c) high-resolution images of crystalline phases in oxidized contact and corresponding FFTs.

The optical transmission $\sim 75\%$ was measured on 120 nm thick ZnO films. For comparison, to yield the same transmission, the Ni/Au metallization had to be thinned down to ~ 15 nm [5], while $\sim 80\%$ transmission was reported for 25 nm thick ITO contacts [6].

The study of the microstructure of GaN/ZnO contact shows two distinct phases at the contact interface, namely Au and ZnO. Since Au does not provide ohmic contact to low-doped p-type GaN, the observed ohmic behavior may be attributed to the formation of n^+ -ZnO. We note

that ohmic characteristics are obtained without any reaction at the metal-semiconductor interface. This in turn implies a lowering of the barrier height at the contact interface. The work function of ZnO is about 5 eV [10], but in view of results reported recently by Klein for degenerately doped In₂O₃ thin films [13], we can expect the formation of a depletion layer in the superficial region of highly doped ZnO. The resultant band bending at the p-GaN/n⁺-ZnO interface in conjunction with high bulk conductivity of ZnO would explain the ohmic properties of this interface.

We expect that the presented ohmic contact technology might be further improved by optimization of the deposition procedure of the nucleation film.

ACKNOWLEDGMENTS

Research is partially supported by grants from European Commission IST-199-10292-AGETHA and the Committee for Scientific Research 7T11B 009 20. TEM group (J.J. and Z. L.-W.) supported by the Director, Office of Science, Office of Basic Energy Sciences, Division of Materials Sciences, of the U.S. Department of Energy under Contract No. DE-AC03-76SF00098 wants to thank W. Swider for TEM sample preparation, and the NCEM in Berkeley for use of the TEM facility.

REFERENCES

1. J.-K. Ho, C.-S. Jong, C.C. Chiu, C.-N. Huang, K.-K. Shih, L.C. Chen, F.R. Chen, and J.-J. Kai, *J. Appl. Phys.* **86**, 4491 (1999).
2. N. Shibata, J. Umezaki, M. Arai, T. Uemura, T. Kozawa, T. Mori and T. Owaki, *Japanese Unexamined Patent No 09064337A*.
3. J.-K. Ho, C.-S. Jong, C.C. Chiu, C.-N. Huang, C.-Y. Chen and K.-K. Shih, *Appl. Phys. Lett.* **74**, 1275 (1999).
4. J.K. Sheu, Y.K. Su, G.C. Chi, P.L. Koh, M.J. Jou, C.M. Chang, C.C. Liu and W.C. Hung, *Appl. Phys. Lett.* **74**, 2340 (1999).
5. J.-S. Jang, S.-J. Park and T.-S. Seong, *J. Appl. Phys.* **88**, 5490 (2000).
6. T. Margalith, O. Buchinsky, D. A. Cohen, A. C. Abare, M. Hansen, S. P. DenBaars and L.A. Coldren, *Appl. Phys. Lett.* **74**, 3930 (1999).
7. Y.-K. Song, M. Diagne, H. Zhou, A. V. Nurmikko, R. P. Schneider, Jr., *Phys. Stat. Sol. (a)* **180**, 33 (2000).
8. Y.R. Ryu, S. Zhu, J. D. Budai, H. R. Chandrasekhar, P. F. Micelli and H. W. White, *J. Appl. Phys.* **88**, 201 (2000).
9. S. B. Qadri, H. Kim, H. R. Khan, A. Pique, J. S. Horowitz, D. Chrisey, W. J. Kim, E. F. Skelton, *Thin Solid Films* **377-378**, 750 (2000).
10. T. Minami, T. Miyata, T. Yamamoto, *Surface and Coating Technol.* **108-109**, 583, (1998).
11. *Handbook of Thin Film Technology*, eds. L.I. Maissel, R. Glang, McGraw-Hill Book Company, (N.Y. 1970).
12. G. K. Reeves, *Solid State Electronics*, **23**, 487 (1980).
13. A. Klein, *Appl. Phys. Lett.* **77**, 2009 (2000).